



Seventh Framework Programme Theme 6 Environment

Collaborative Project (Large-scale Integrating Project)

Project no. **212085**

Project acronym: **MEECE**

Project title: **Marine Ecosystem Evolution in a Changing Environment**

D2.2 Sub-model acidification-sensitive calcification rate, including user guide

Due date of deliverable: 31.05.09

Actual submission date: 05.05.09 updated 16.02.10

Organisation name of lead contractor for this deliverable: PML

Start date of project: 01.09.08 Duration: 48 months

Project Coordinator: Icarus Allen, Plymouth Marine Laboratory

Project co-funded by the European Commission within the Seventh Framework Programme, Theme 6 Environment		
Dissemination Level		
PU	Public	x
PP	Restricted to other programme participants (including the Commission)	
RE	Restricted to a group specified by the consortium (including the Commission)	
CO	Confidential, only for members of the consortium (including the Commission)	



D2.2 Sub-model acidification-sensitive calcification rate, including user guide

Jerry Blackford, Yuri Artioli (PML), Boris Kelly-Gerreyn, Adrian Martin and Toby Tyrrell, (National Oceanography Centre, Southampton), Raquel Somavilla (IEO-Santander)

Delivered 5th May 2009
Updated 16th February 2010.

Table of Contents

SECTION 1. THE CARBONATE SYSTEM USER GUIDE	2
1.1 Introduction	2
1.2 The Carbonate System	2
1.2.1 Implementation	4
1.3 Air – Sea exchange of CO₂	7
1.3.1 FORTRAN Code	7
1.4 Model Code	9
SECTION 2. CALCIFICATION MODEL USER GUIDE	10
2.1 Introduction	10
2.1.2 Towards a new model of calcification: considerations from the literature	12
2.2 Implementation	14
2.2.1 Intercomparison of Calcification Parameterisations	15
2.2.2 Inter-comparison of calcification parameters	18
SECTION 3. OCEAN ACIDIFICATION SENSITIVITIES AND IMPACTS	28
3.1 Introduction	28
3.2 Nitrification	28
3.3 Calcification	28

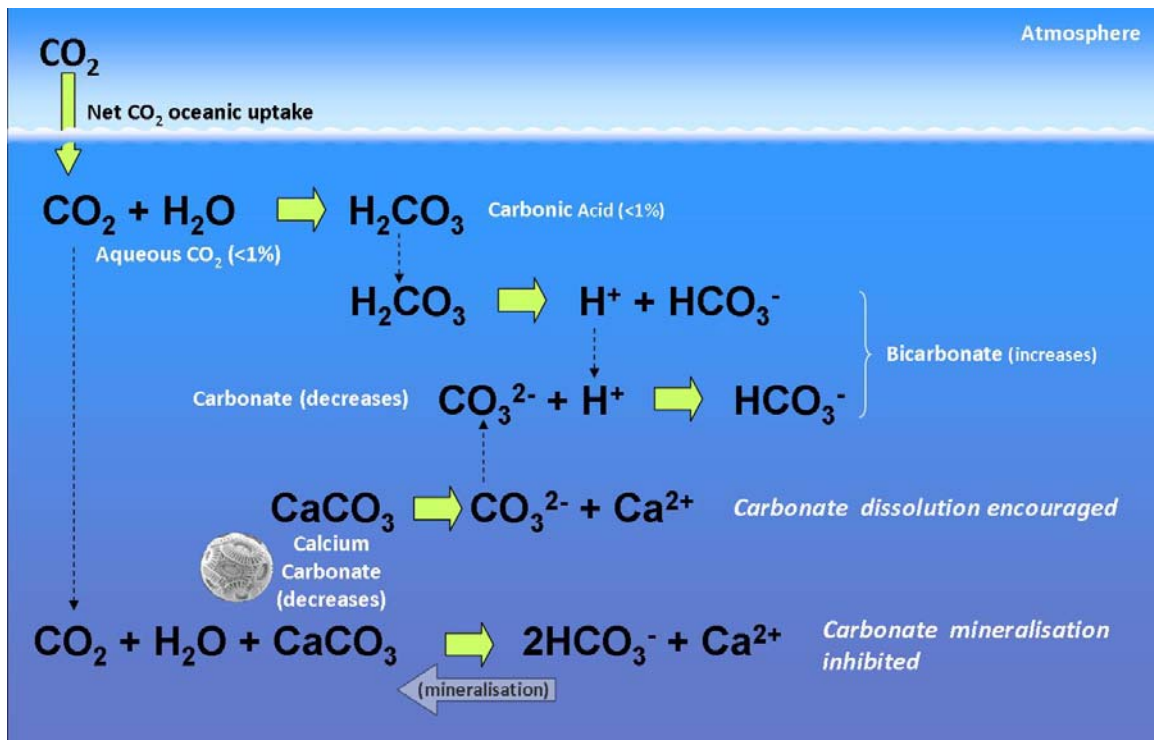
This user guide consists of three parts:

Section 1: A guide to implementing the carbonate system in NPZD type models, which is a necessary precursor for defining sensitivity to ocean acidification.

Section 2: A user guide describing the incorporation of the process of calcification into models.

Section 3: A short section that discusses process sensitivity to acidification.

This user guide/manual, along with links to the necessary code and interface variables, is available in full at <http://www.meece.eu/Library.aspx>



A summary of the key chemical reactions that occur when CO₂ is added to the marine system (the carbonate system) and the potential consequences for calcification.

Section 1. The Carbonate System user guide.

(Jerry Blackford & Yuri Artioli, Plymouth Marine Laboratory)

1.1 Introduction

The carbonate system refers to the chemical processes that describe the behaviour of CO₂ when dissolved in seawater. There are two aspects to determining the carbonate system in marine models. Firstly the calculation of the partition of CO₂ within the carbonate system and secondly the calculation of the rate of exchange of CO₂ across the air-sea interface.

The geochemistry of ocean acidification is based on a very well defined understanding (e.g. Zeebe & Wolf-Gladrow, 2001) and the availability of internationally agreed carbonate chemistry equations enables a consistent, robust approach, even if there is some remaining uncertainty about constants. The carbonate system is defined by four analytically determinable master variables, total or dissolved inorganic carbon (DIC), total alkalinity TA, the partial pressure of CO₂ in water (pCO_{2w}) and pH. Knowledge of any two of these along with basic physical properties is sufficient to derive the other two and the carbonate saturation state omega (Ω), bicarbonate concentration ([HCO₃⁻]) and carbonate concentration ([CO₃²⁻]). From pCO_{2w}, the equivalent atmospheric measurement and wind speed it is possible to calculate air-sea CO₂ flux and hence identify sources and sinks of CO₂. Typically models use calculated total inorganic carbon and a parameterisation of total alkalinity to drive the carbonate equations and derive pH and pCO₂. For open ocean situations the derivation of alkalinity from modelled salinity is a reasonable first approximation (Millero et al., 1998; Lee et al., 2006) although biological activity can modify the alkalinity significantly. Unfortunately dealing with alkalinity in such heterogeneous environments is far more problematic than in oceanic systems as the linear relationships with salinity break down (Bellerby et al, 2005; Thomas et al, 2009).

The principle uncertainties in modelling spatial and temporal variability in the carbonate system and accurately predicting ocean acidification relate to coastal and shelf environments and their boundaries. Riverine input of dissolved inorganic carbon and alkalinity is poorly monitored but significant in, for example, coastal regions of the North Sea (Thomas et al, 2005b, Pätsch & Lenhart, 2004, Seitzinger et al, 2005). Riverine alkalinity cannot be assumed to be constant over time, for example changing rainfall and land use patterns have increased the alkalinity of the Mississippi by >50% over the last half century (Raymond & Cole, 2003). Estuarine systems are in themselves complex with daily and seasonal dynamics (Borges & Frankignoulle, 1999), with a need for individual parameterisations of gas transfer velocities (Borges et al, 2004) and significant net CO₂ emissions (Frankignoulle et al, 1998). These and other issues are summarized in Blackford (2010).

1.2 The Carbonate System

When CO₂ dissolves in seawater it combines with water molecules to form carbonic acid, (H₂CO₃), which rapidly dissociates into bicarbonate ions (HCO₃⁻) and protons (H⁺). Some of the protons combine with carbonate ions (CO₃²⁻) to form more bicarbonate (the carbonate buffer), whilst the remaining hydrogen ions increase the acidity (lowering the pH) of the water (figure 1.). These processes can be considered to occur instantaneously for modelling purposes. The process is moderated by the alkalinity content of seawater (approximately the sum of weakly bound negatively charged ions including carbonate and bicarbonate). The carbonate system is described in detail in many publications, (e.g. Andersson et al 2006 for an introductory text, Zeebe and Wolf-Gladrow, 2001 for a detailed description).

For the purposes of modelling the carbonate system the important fact to know is that two from the four analytically determinable quantities of the carbonate system need to be known a-priori for the remaining quantities of the carbonate system to be calculated along with basic hydrographical information such as temperature and salinity.

Quantity	Abbreviation	Units
Dissolved Inorganic Carbon or Total Inorganic Carbon	DIC / T _C	µmol.kg ⁻¹
Total alkalinity	TA / T _{alk}	µmol.kg ⁻¹
The partial pressure of CO ₂ in the water	p CO ₂ w	µatm
-log [hydrogen ions]	pH	pH

Table 1: Four master variables of the carbonate system

The equations and coefficients that govern this derivation have been described comprehensively elsewhere (for example see chapter 2 of the Guide to Best Practices for Ocean CO₂ Measurements, 2007) and are unnecessary to repeat here.

The recommended and simplest method of incorporating the carbonate system in an existing model is to insert a call to one of a selection of available routines (see below) into the main programme loop (e.g. at each timestep and spatial node). The majority of models (in the MEECE context) will approach the carbonate system by calculating DIC within the host biogeochemical / ecosystem model as a product of respiration and photosynthesis. The second required variable is generally alkalinity. As alkalinity is conservative it can be approximated from salinity for the open ocean, however each region has its own formulation (see table 2) and biological activity (e.g. Coccolithophore blooms in the N. Atlantic) can significantly alter in-situ alkalinity. The current ERSEM approach – see below – might also be appropriate for open ocean systems. Equations for open ocean alkalinity are described in (Millero et al., 1998 and Lee et al. 2006).

Basin	Formula	Reference
Nordic, N Atlantic	TA = 66.960*S - 36.8	Bellerby et al 2005
Atlantic Ocean	TA = 51.240*S + 520.1	Millero 1998
Pacific Ocean	TA = 54.629*S + 399.0	Millero, 1998
Indian Ocean	TA = 68.800*S - 114.0	Millero, 1998

Table 2: Example equations for deriving alkalinity from salinity.

A more sophisticated approach is required in highly dynamic, riverine influenced shelf and coastal systems. The ideal approach for shelf systems is to describe alkalinity as a separate state variable which takes the form of a function of background alkalinity, riverine alkalinity nutrient processes and the carbonate cycle (the mineralization and dissolution of calcium carbonate). However it is still possible to use a simple function of salinity (as in Blackford & Gilbert 2007), as long as the resulting errors are considered.

The current ERSEM model is developing a model of alkalinity of the form:

$$\begin{aligned}
 &Talk = f(s) \\
 &+/- f(\text{biological nutrient uptake/loss}) \\
 &+/- f(\text{biogenic carbonate precipitation / dissolution}) \\
 &+/- f(\text{riverine input})
 \end{aligned}$$

Integration of this more sophisticated model is dependant on the model information available, especially the inclusion of calcification and the availability of riverine data if appropriate.

A number of coded options for determining the carbonate system exist, providing applications to suit most parent ecosystem codes.

1.2.1 Implementation

FORTRAN routines as implemented in the ERSEM model

The existing ERSEM model contains code which can simulate carbonate system variables (total alkalinity, dissolved inorganic carbon, pH, pCO₂ etc) in shelf seas for present and future atmospheric CO₂ scenarios (Blackford & Gilbert 2007). The file *CO2_dyn.F90* contains a set of FORTRAN subroutines that calculate the carbonate system at any given point in marine space time, given values for temperature, salinity, DIC, depth (pressure). This is essentially an implementation of the Haltafall speciation code (Ingri et al 1967). The code has been developed by Jerry Blackford and others at PML. Outputs are values for: total alkalinity, pH, partial pressure of CO₂ in water, carbonate and bicarbonate ion concentrations, and calcite and aragonite calcification states. The code is supplied with a programme 'wrapper' that provides a stand alone implementation capability.

The code supplied can be implemented by inserting the following call in an appropriate position in the existing model:

```
Call CO2 dynamics (Temperature, Salinity, Depth, DIC, pco2w, TA, ph,
cco2, carba, bicarb, carb, henry, om_cal, om_arg, tCO2, dcf)
```

Where, temperature (°C), salinity (psu), depth (metres) and DIC (mmol.m⁻³), must be defined beforehand. The routines convert from mmol.m⁻³ to μmol.kg⁻¹, which is the unit used within the carbonate system calculation. **Within the CO₂ routines supplied a formulation for alkalinity must be coded.**


The routine outputs:


DIC	dissolved inorganic carbon in units of μmol.kg ⁻¹
pCO _{2w}	the partial pressure of CO ₂ in seawater (μatm)
pH	-log [hydrogen ions] (pH)
carba	concentration of carbonic acid (mmol.m ⁻³)
bicarb	bicarbonate ion concentration (mmol.m ⁻³)
carb	carbonate ion concentration (mmol.m ⁻³)
henry	the value of henry's constant (at given temperature)
om_cal	the saturation state (Ω) with respect to calcite
om_arg	the saturation state (Ω) with respect to aragonite

Reference for prior usage of this code: Blackford & Gilbert, 2007. Contact Jerry Blackford, jcb@pml.ac.uk for advice regarding implementing this code.

Alternative applications for determining carbonate chemistry.

Many other packages exist, replicating the same functionality in different languages. Each of these packages are fully documented on their respective web sites.

	<p>CO₂Sys: by Ernie Lewis & Doug Wallace http://cdiac.ornl.gov/oceans/co2rprt.html</p> <p>Provides code suitable for Excel & Matlab system</p>
---	--

	<p>SWCO₂: by Keith Hunter http://neon.otago.ac.nz/research/mfc/people/keith_hunter/software/swco2/</p> <p>Provides code formatted as a dynamic link library suitable for Microsoft Office applications, Visual Basic, Visual C++, Borland Delphi or MatLab systems.</p> <p>This site also provides a useful stand alone windows executable called CO₂Calc which provides an excellent platform for exploring the behaviour of the carbonate system</p>
---	--

General application and pitfalls of using carbonate system models

Although the carbonate system is well understood there are other issues, in addition to those already discussed concerning alkalinity, that require mention.

- **The first** is that a number of definitions of the pH scale exists, dependant on the method of determination used. The only two that are appropriate to use for marine systems are the **total scale** or the **seawater scale**.
- **Secondly** a number of sets of equilibrium constants that govern the carbonate equations have been published resulting from various studies. There is no universally accepted set of coefficients for ocean acidification however the recommendation is to use the Mehrbach (1973) constants as refitted by Dickson & Millero (1987). These have the advantage of being derived from natural as opposed to artificial seawater and importantly are used in the OCMIP studies.
- **Thirdly** it is important to ensure that the correct units are used. The carbonate system routines generally use $\mu\text{mol.kg}^{-1}$ (of seawater) whilst biogeochemical ecosystem models generally define concentrations in units of mmol.m^{-3} or the equivalent $\mu\text{mol.l}^{-1}$. Although a concentration expressed in $\mu\text{mol.kg}^{-1}$ only differs by $\sim 2.5\%$ from the same expressed in mol.m^{-3} , depending on water density, this difference is hugely significant when determining the carbonate system.

The potential error that may arise from using the wrong units or inappropriate constants and pH scales is illustrated below.

Inputs (T=5, S=35)				
Constant set		Mehrbach, refit by Dickson and Millero	Hansson, refit by Dickson and Millero	Mehrbach, refit by Dickson and Millero
DIC	?	2100 $\mu\text{mol.kg}^{-1}$	2100 $\mu\text{mol.kg}^{-1}$	2100 (mmol.m^{-3})
TA	$\mu\text{mol.kg}^{-1}$	2300	2300	2300
Outputs				
pH tot	pH	8.163225	8.14685	8.278721
pH sws	pH	8.155689	8.139314	8.271185
pH free	pH	8.21429	8.197915	8.329786
pH nbs	pH	8.257918	8.241543	8.373414
H ₂ CO ₃	$\mu\text{mol.kg}^{-1}$	14.96833	15.98673	10.95679
HCO ₃	$\mu\text{mol.kg}^{-1}$	1942.992	1938.699	1855.568
CO ₃	$\mu\text{mol.kg}^{-1}$	142.0396	145.3138	176.9748
pCO ₂	μatm	288.3145	307.9306	211.0456
Omega-C	~	3.390122	3.468269	4.223936
Omega-A	~	2.140588	2.189931	2.667074

Table 3: Variability of results dependant on units, pH scale and constants used. Black represents correct calculations, red for errors.

Recommended definitions of constants

K0 from Weiss 1974

$$k_0 = \exp(93.4517 / (tk/100.0) - 60.2409 + 23.3585 * \log(tk/100.0) + s * (.023517 - 0.023656 * (tk/100.0) + 0.0047036 * (tk/100.0)^2))$$

k1 = [H][HCO₃]/[H₂CO₃], k2 = [H][CO₃]/[HCO₃], from Millero p.664 (1995) using Mehrbach et al. data on seawater scale

$$k_1 = 10^{**}(-1*(3670.7/TK - 62.008 + 9.7944*\ln(TK) - 0.0118 * s + 0.000116*s^2))$$

$$k_2 = 10^{**}(-1*(1394.7/TK + 4.777 - 0.0184*S + 0.000118*S^2))$$

kb = [H][BO₂]/[HBO₂] from Millero p.669 (1995) using data from Dickson (1990)

$$K_b = \exp((-8966.90 - 2890.53*\sqrt{S} - 77.942*S + 1.728*S^{1.5} - 0.0996*S^2) / TK + (148.0248 + 137.1942*\sqrt{S} + 1.62142*S) + (-24.4344 - 25.085*\sqrt{S} - 0.2474*S) * \ln(TK) + 0.053105*\sqrt{S}*TK)$$

TK = temperature in kelvins, S = salinity, psu

Conversion between mmol.m⁻³ and μmol.kg⁻¹

The recommended calculation for seawater density (kg.m⁻³) at the prevailing temperature (T, °C) and salinity (S, psu) is Millero & Poisson, Deep-Sea Research, 1981, (aka UNESCO, 1981) with T: Temperature in degree Celsius; S: Salinity in practical units, valid for 0<T<40 and 0.5<S<43.

$$a = 8.24493d-1 - 4.0899d-3*T + 7.6438d-5*T**2 - 8.2467d-7*T**3 + 5.3875d-9*T**4$$

$$b = -5.72466d-3 + 1.0227d-4*T - 1.6546d-6*T**2$$

$$c = 4.8314d-4$$

Density = (999.842594 + 6.793952d-2*T- 9.095290d-3*T**2 + 1.001685d-4*T**3 - 1.120083d-6*T**4 + 6.536332d-9*T**5+a*S+b*S**1.5+c*S**2)

Density conversion factor = density / 1000.0
 X (umol/kg) = X (mmol/m3) / dcf

Inputs					
Temperature	°C	25	5	25	5
Salinity	psu	35	35	35	35
Depth	m	0	0	0	0
DIC	mmol.m ⁻³	2000	2100	2100	2200
DIC	μmol.kg ⁻¹	1954.379	2043.447	2052.098	2140.754
TA	μmol.kg ⁻¹	2300	2300	2300	2300
Outputs					
pH	pH	8.125	8.277	7.956	8.066
pCO _{2w}	μatm	307.990	206.947	496.904	363.480
Carbonic acid	mmol.m ⁻³	8.948	11.087	14.437	19.472
Bicarbonate	mmol.m ⁻³	1734.833	1904.637	1895.897	2058.030
Carbonate	mmol.m ⁻³	256.219	184.276	189.666	122.498
calcite	~	6.024	4.278	4.459	2.844
aragonite	~	3.971	2.701	2.939	1.796

Table 4. Reference check data for code implementation.

1.3 Air – Sea exchange of CO₂

This is driven by the difference in partial pressure of CO₂ between the two mediums. Atmospheric pCO₂ (pCO_{2a}) is relatively constant across an annual cycle, although some spatial heterogeneity exists at global scales relating to the location of industrial and population sources. Increased anthropogenic CO₂ is currently causing a rise of pCO_{2a} by about 2 µatm per year. The unit is sometimes referred to as µatm, sometimes as ppm. These are equivalent.

Example values of pCO₂ in the atmosphere

Glacial minimum	180
Pre-industrial / glacial maximum	280
Year 2000	375
Predicted for year 2100*	700

*Future predictions are dependant on emission scenario, see Caldeira and Wickett, 2003.

Seawater pCO₂ (pCO_{2w}) is influenced by physical processes (temperature) and biological processes, (primary production and respiration). Consequently pCO_{2w} exhibits a strong annual cycle, depending on environment, which results in reversal of air-sea CO₂ flux according to the time of year. (See Thomas et al, 2005 for description of pCO_{2w} on the NW European shelf.).

1.3.1 FORTRAN Code

The ERSEM model contains a routine that calculates oceanic out-gassing / take-up of CO₂ given a time-varying parameterization of atmospheric pCO₂ (pCO_{2a}), which if coupled with the carbonate system model allows the determination of acidification driven by atmospheric CO₂.

The routine, as supplied in this deliverable, is a stand alone routine, the call to which should be inserted in the main loop after the call to the carbonate system and **only for the surface boxes**.

For surface boxes only

```
Call Air_sea_exchange (Temperature, WindSpeed, pCO2w, pCO2a, Henry,
dcf, flux)
```

```
DIC = DIC + flux * dcf
```

The pre-defined inputs are temperature, wind speed in metres per second, pCO_{2w} (calculated by the carbonate system), pCO_{2a} (defined as a time varying parameter in a suitable external data file), the value of henry's constant (also from the carbonate system call). The output is the air-sea flux of DIC/CO₂ which should be **applied to the state variable for DIC in the model**, ensuring appropriate units. The convention is that a positive flux is an uptake by the marine system, a negative flux represents out gassing. (Note that climate models use the opposite convention.)

The code uses the the Nightingale and Liss parameterisation for gas transfer velocity

Reference for prior usage of this code: Blackford & Gilbert, 2007. J Mar Sys 64, 229-241.

References

- Andersson, A.J., Mackenzie, F.T., Lerman, A., 2006. Coastal ocean CO₂-carbonic acid-carbonate sediment system of the Anthropocene. *Global Biogeochemical cycles*, 20, GB1S92.
- Bellerby R.G.J., Olsen A., Furevik T., Anderson L.A., 2005. Response of the surface ocean CO₂ system in the Nordic Seas and North Atlantic to climate change. In: Drange, H., Dokken, T.M., Furevik, T., Gerdes, R., Berger, W. (Eds.), *Climate Variability in the Nordic Seas: Geophysical Monograph Series*, AGU, pp. 189–198.
- Blackford J.C., Gilbert F.J., 2007. pH variability and CO₂ induced acidification in the North Sea. *Journal of Marine Systems* 64, 229–241.
- Blackford, J.C., 2010. Predicting the impacts of ocean acidification: Challenges from an ecosystem perspective, *Journal of Marine Systems*, doi:[10.1016/j.jmarsys.2009.12.016](https://doi.org/10.1016/j.jmarsys.2009.12.016)
- Borges A.V., Frankignoulle M., 1999. Daily and seasonal variations of the partial pressure of CO₂ in surface seawater along Belgian and southern Dutch coastal areas. *Journal of Marine Systems* 19, 251–266.
- Borges, A.V., Delille B., Schiettecatte L.-S., Gazeau F., Abril G., Frankignoulle M., 2004. Gas transfer velocities of CO₂ in three European estuaries (Randers Fjord, Scheldt, and Thames). *Limnology & Oceanography*, 49(5), 1630–1641.
- Caldeira K., Wickett, M.E., 2005. Ocean model predictions of chemistry changes from carbon dioxide emissions to the atmosphere and ocean. *J Geophysical Research* 110, C09S04.
- Dickson, A.G. Millero, F.J., 1987. A comparison of the equilibrium constants for the dissociation of carbonic acid in seawater media. *Deep-Sea Res.* **34**, 1733–1743. (Corrigenda. *Deep-Sea Res.* **36**, 983).
- Dickson, A.G. 1990b. Thermodynamics of the dissociation of boric acid in synthetic sea water from 273.15 to 298.15 K. *Deep-Sea Res.* **37**: 755–766.
- Frankignoulle, M., Abril, G., Borges, A., Bourge, I., Canon, C., DeLille, B., Libert, E., Theate, J.M., 1998. Carbon dioxide emission from European estuaries, *Science*, 282, 434–436.
- Dickson, A.G., Sabine, C.L., Christian, J.R., (Eds), 2007. Guide to best practices for ocean CO₂ measurements. PICES special publication 3, 191 pp. http://cdiac.ornl.gov/oceans/Handbook_2007.html
- Ingri, N., Kakolowicz, W., Sillén, L.G., Warnqvist, B., 1967. Highspeed computer as a supplement to graphical methods: V. HALTAFALL, a general program for calculating the composition of equilibrium mixtures. *Talanta* 14, 1261.
- Lee, K., Tong, L.T., Millero, F.J., Sabine, C.L., Dickson, A.G., Goyet, C., Park, G.H., Wanninkhof, R., Feely, R.A., Key, R.M., 2006. Global relationships of total alkalinity with salinity and temperature in surface waters of the world's oceans, *Geophysical Research Letters*, 33, L19605.
- Mehrbach, C., Culbertson, C.H., Hawley, J.E. and Pytkowicz, R.M. 1973. Measurement of the apparent dissociation constants of carbonic acid in seawater at atmospheric pressure. *Limnol. Oceanogr.* **18**: 897–907.
- Millero, F.J. 1995. Thermodynamics of the carbon dioxide system in the oceans. *Geochim. Cosmochim. Acta* **59**: 661–677.
- Millero, F.J., Lee, K., Roche, M., 1998. Distribution of alkalinity in the surface waters of the major oceans. *Marine Chemistry* 60, 111–130.
- Nightingale, P.D., Malin, G., Law, C.S., Watson, A.J., Liss, P.S., Liddicoat, M.I., Boutin, J., Upstill-Goddard, R.C., 2000. In situ evaluation of air–sea gas exchange parameterizations using novel conservative and volatile tracers. *Global Biogeochemical Cycles* 14, 373–388.
- Pätsch, J., Lenhart, H.J., 2004. Daily Loads of Nutrients, Total Alkalinity, Dissolved Inorganic Carbon and Dissolved Organic Carbon of the European Continental Rivers for the Years 1977–2002. *Berichte aus dem Zentrum für Meeres- und Klimaforschung; Reihe B: Ozeanographie*, 48, 159 pp.
- Raymond P.A., Cole J.J., 2003. Increase in the Export of Alkalinity from North America's Largest River. *Science* 301, 88–91.
- Seitzinger, S. P., Harrison, J. A., Dumont, E., Beusen, A. H. W., Bouwman, A. F., 2005. Sources and delivery of carbon, nitrogen, and phosphorus to the coastal zone: An overview of Global Nutrient Export from Watersheds (NEWS) models and their application, *Global Biogeochemical Cycles*, 19, GB4S01.
- Thomas, H., Bozec, Y., Elkalay, K., de Baar, H. J. W., Borges, A. V., Schiettecatte, L.-S. 2005b. Controls of the surface water partial pressure of CO₂ in the North Sea, *Biogeosciences*, 2, 323–334.
- Thomas, H., Schiettecatte, L.-S., Suykens, K., Koné, Y. J. M., Shadwick, E. H., Prowe, A. E. F., Bozec, Y., Baar, H. J. W. de, Borges, A. V., 2009. Enhanced ocean carbon storage from anaerobic alkalinity generation in coastal sediments. *Biogeosciences*, 6, 267–274.
- Weiss, R.F., 1974. Carbon dioxide in water and seawater: the solubility of a non-ideal gas. *Marine Chemistry* 2, 203–215.

Zeebe, R.E., Wolf-Gladrow, D.A., 2001. CO₂ in seawater: equilibrium, kinetics and isotopes. Elsevier Oceanography Series 65, 346.

1.4 Model Code

Contact the model developers for the latest version of the code :

Jerry Blackford, Yuri Artioli (PML), Boris Kelly-Gerreyn, Adrian Martin and Toby Tyrrell, (National Oceanography Centre, Southampton), Raquel Somavilla (IEO-Santander)

Section 2. Calcification model user guide.

Boris Kelly-Gerreyn, Adrian Martin and Toby Tyrrell, (National Oceanography Centre, Southampton), Raquel Somavilla (IEO-Santander)

Summary

This document describes a new algorithm for calculating acidification-sensitive pelagic calcification rate. Here we review previous algorithms for pelagic calcification, as reported in various published articles, as used in different ecosystem/biogeochemical models. We also review the experimental/observational literature on how calcification rate depends on environmental conditions, and come up with a new recommended formulation as to how to represent calcification in the MEECE models. Furthermore, we test the new formula as well as the previous formulae in a new 0-D model written for the purpose. This model is an NPZD plankton model for the Bay of Biscay, encompassing nutrients, plankton, detritus and carbonate chemistry. The NPZD part of the model is optimised to give a good fit to nutrient and chlorophyll data for the region, and then alternative calcification routines are bolted on top. We then compare model results to carbonate chemistry data for this location. The ability of the different formulae to reproduce the observed seasonal patterns of dissolved inorganic carbon (DIC) and alkalinity at this location is examined.

2.1 Introduction

An overview of marine pelagic calcification equations

Models of marine pelagic calcification fall into three categories (Table 1): those that 1) multiply rates of primary production by a factor which may be fixed (e.g. Buitenhuis et al 2001, Joassin et al 2008) or variable (e.g. Moore et al 2002, Aumont and Bopp 2006, Gehlen et al 2007), 2) multiply the export flux out of the euphotic layer by the so-called rain ratio (e.g. Ridgwell et al 2007, Zahariev et al 2008) and 3) model calcite production directly from the phytoplankton biomass (e.g. Tyrrell and Taylor 1996, Merico et al 2004). All model equations are shown in Table 1.

Category 1 models: Calcification based on primary production

Moore et al (2002) developed a global biogeochemical model in which calcite production was a variable fraction (centred around 0.05, taken from Balch et al 2000) of the rate of gross primary production of small phytoplankton. This fraction was modulated by nutrient limitation, temperature and the concentration of small phytoplankton (equation 1a, Table 1). Moore et al (2002) justified their approach by suggesting that observed ratios of calcification to photosynthesis (C:P) are low in oligotrophic waters (hence the use of the square of the nutrient limitation term, equation 1b), that there are latitudinal gradients in calcification (hence the use of different temperature-dependent formulae for the temperature function, equations 1c-e) and that blooms of small phytoplankton are often dominated by coccolithophores (hence the use of the $P_{small}/2$ term, equation 1a). However, there was no clear justification given for the parameter values associated with the temperature function (1c-d) and the small phytoplankton concentration (1a). Aumont and Bopp (2006) adopted the approach of Moore et al (2002) to model calcification in another global ocean model (called PISCES), but replaced the fraction parameter (C_f , equation 1a) with the cellular PIC:POC ratio¹ (equation 2a, 2c). This ratio was calculated from a maximum PIC:POC ratio and modulated by nutrients, temperature and small phytoplankton concentrations (equation 2a) in a similar way to Moore et al (2002). However, Aumont and Bopp (2006) did not square the nutrient limitation term and they modified both the temperature function and the threshold level (from 2 to 1) above which small phytoplankton concentrations raise the calcification rate (2a). No justification for these changes was presented. The PIC:POC ratio was constrained to fall between 0.01 and 0.8.

¹ Aumont and Bopp (2006) referred to this as the rain ratio

Gehlen et al (2007) added a limitation function based on the saturation state (Ω) to the PISCES model (equation 3a) to address the changes in pelagic calcite production in response to rising atmospheric CO₂ levels. The limitation function for the saturation state was derived from experimental data under nutrient replete conditions, in which a Michaelis-Menten type function was imposed relating PIC:POC ratios to $\Omega-1$.

Le Quere et al (2005) developed the Dynamic Green Ocean Model (DGOM) and used a constant C:P ratio (0.433) derived from Buitenhuis et al (2001) to calculate calcification from coccolithophorid primary production (4a). Similarly, Fujii and Chai (2007) used a constant cellular PIC:POC ratio (=1) to calculate calcification from gross primary production of coccolithophorids (5a) in a 3-D model of the equatorial Pacific. The choice of value for their PIC:POC ratio was not fully justified. The only study (Joassin et al, 2009) to model data from a mesocosm experiment (Delille et al 2005), expressed calcification as the product of net primary production and the PIC:POC ratio (=0.58, derived from the mesocosm data) as well as an additional term which accounts for a basal rate of calcification (equation 6a). The latter was a function of *E. huxleyi* biomass and a first order rate constant ($C_{basalrate}$) derived from the data. This additional term effectively decoupled calcification from photosynthesis.

Heinze (2004) and Ilyina et al (2008) used the HAMOCC global biogeochemical model to calculate the flux of calcite out of the euphotic zone. The Heinze (2004) formula (equation 7a) involves a free tunable parameter (A), akin to the PIC:POC ratio or C_f (equation 1a), and the difference between total primary production and biogenic silica production. The reason for this formula is unclear, but is related to the idea that “Production of siliceous plankton shell material is preferentially carried out in areas of significant silicic acid supply to the surface ocean.” (Heinze, 2004) and that “Export of calcite and opal particles are steered by the availability of dissolved Si.” in the model (Ilyina et al 2008). Heinze (2004) also included a term (7b,c) derived from laboratory experiments (Zondervan et al 2001) for investigating the impact of rising atmospheric CO₂ concentrations on calcification rates. Ilyina et al (2008) added a parameter r to equation 7a, which they referred to as a rate coefficient. However, such terminology seems inappropriate given that their equation (8a) contains the primary production term. The value of r was given different functional forms (linear, parabolic and hyperbolic) dependent on Ω .

Friis et al (2008) combined a spatially varying rain ratio (derived from Sarmiento et al 2002) with phosphate-limited primary production² to model calcite export production (9a,b). Buitenhuis et al 2001 developed a 1D (3 layer) model to describe field and mesocosm data. Their calcification equation (10a) is the product of a fixed CP ratio (0.42) derived from the data, the biomass of *Emiliana huxleyi* and a time-dependent first order calcification (growth) rate constant (k_{calcif}). The latter was parameterised with a time delay (2 days) to account for observations showing the continuation of calcification after photosynthesis became nutrient limited.

Category 2 models: calcification modelled from the export flux

Zahariev et al (2008) developed a global model (Canadian Model of Ocean Carbon, CMOC) in which the biogenic calcite export flux (11a) was a function of a temperature dependent rain ratio (11b). The temperature function gives a logistic curve varying from 0 to 1 with the largest gradient between 5°C and 15°C, which is the temperature range in which the largest blooms of coccolithophores occur (Iglesias-Rodriguez et al 2002). Zahariev et al (2008) refer to an unpublished Norwegian PhD thesis (Drange, 1994) to justify their approach. The PIC flux is further modified such that it decreases with depth (11c) according to a predefined “re-dissolution” length scale (d_{PIC} , Table 2).

Ridgwell et al (2007) used GENIE-1 to calculate the rain ratio (equation 11a) from the product of a spatially-uniform rain ratio scalar (equation 12b) and a function of the local surface ocean

² Friis et al (2008) refer to this as net primary production

saturation state (Ω), termed a thermodynamically based modifier of the rate of carbonate production.

Category 3 models: direct modelling of calcification from phytoplankton biomass

Tyrrell and Taylor (1996) modelled calcification (equation 13a) in the north Atlantic as a function of *Emiliana huxleyi* biomass, temperature, light and a maximum rate of coccolith production (C_{max}). This model has been used in other modelling studies since (Merico et al 2004, Findlay et al 2008). The half saturation constant for light ($I_{h,d}$) is assumed to be half the corresponding value for *Emiliana huxleyi* growth, an assumption which is supported by studies showing that calcification is less light limited than photosynthesis (Zondervan et al 2007). The light used is PAR, justified by a single study (Paasche, 1966) in which absorption peaks for both calcification and photosynthesis occurred at the same red and blue wavelengths. However, as suggested by Paasche (2002), further experimental studies are needed to confirm these light dependencies.

2.1.2 Towards a new model of calcification: considerations from the literature

Phosphate

Phosphate limitation and to a lesser degree nitrate limitation enhances calcification (Paasche, 1998, Riegman et al 2000, Muller et al 2008). This is in contrast to the lowering of calcification under iron limitation (Schulz et al 2004). In the case of reduced phosphate concentrations, abnormal coccoliths may be produced (Andersen, 1981; Paasche, 1998). One possible reason why phosphate limitation enhances calcification may be to do with an as yet unidentified phosphorus-based inhibitor for calcification (Andersen, 1981). A particularly compelling argument (Muller et al 08) suggests that calcification can only occur in a particular phase of the cell cycle (the non-dividing nutrient uptake phase, or the assimilation phase commonly termed G1). Corroborative evidence for this comes from Balch et al (1991) who measured maximum calcification rates and coccolith production during the logarithmic phase of the cell cycle - the phase of maximum nutrient assimilation. Muller et al (2008) suggest that the lack of phosphorus may prolong the cell in the G1 phase, because the subsequent DNA replication (S phase) and cell division (G2+M) phases are reliant on phosphorus (more than nitrogen). Furthermore, the cell constituents responsible for calcite formation are in the process of being destroyed and regenerated in the S and G2+M cell phases, suggesting that calcification can only take place in the G1 phase. Presumably, this applies to other cell processes including photosynthesis, but unlike these processes, calcification is not directly reliant on nutrients. Interestingly, the continuation of calcification (PIC production) following the main peak in the coccolithophorid bloom in mesocosm experiments (Delille et al 2005, Schulz et al 2008) is a period of above Redfield N:P ratios (both inorganic and organic). Calcification has also been observed to continue following a decline in photosynthesis in batch culture experiments (see Buitenhuis et al 2001). If the G1-calcification hypothesis holds, then the post-peak period in these various experiments may be a non-dividing phase of the coccolithophore cells, which prolongs calcification beyond the peak of the bloom. Under these conditions, it is likely that cell size would continue to increase. In contrast, under non-limiting nutrient and light conditions, Muller et al (2008) found that once the cell reached a particular size (5 μ m diameter), the cell left the G1 phase. Although the work by Muller et al (2008) needs to be corroborated by further studies, the cell cycle hypothesis provides mechanistic underpinning for previous studies showing the role of phosphate in calcification (see Paasche 2002), making it an attractive idea for a new parameterisation of calcification.

Temperature

Global satellite-based distributions of coccolithophorids suggest that calcifying planktonic organisms are most abundant in a temperature range of 5°C to 15°C (Iglesias-Rodriguez et al 2002). This suggests an optimum temperature for calcification, although it should be kept in mind that satellite distributions are biased towards surface blooms and in fact coccolithophores comprise a sizeable fraction of total biomass in most warm tropical and sub-tropical oceans.

However, the role of temperature is unclear. Watabe and Wilbur (1966) showed that there may be a temperature optimum for calcification in the temperature range 7°C - 27°C, but Paasche (1968) showed no such relationship, whose study, unlike Watabe and Wilbur's, was based on a monoculture. Paasche (1968) thus suggested that Watabe and Wilbur's results may reflect the different dominance of naked and shelled cells at different temperatures in their experiment. Feng et al (2008) also found no relationship between temperature and calcification but their study was restricted to higher temperatures (20 and 24). In contrast, Langer et al (2007) measured a five fold increase in calcification over a wider range in temperature (5°C -15°C), after which there was no further increase (to 20°C). Hence, calcification may be maximal beyond a certain temperature, helping to explain the lack of a temperature response in Feng et al (2008). To complicate matters, Sorrosa et al (2005) found that calcification was higher at lower temperatures (10°C vs. 20°C) after a period of 150 hours in incubation. Consequently, differences in the temperature response by coccolithophorids in these studies may be due to differences in strain. Given that temperature is an important control on the growth and nutrient uptake rates of phytoplankton, and that calcification rates are highest during the main growing season, it seems reasonable to include temperature when modelling calcification. Introducing a threshold temperature beyond which temperature ceases to have an effect on calcification rates (after Langer et al 2006 and Feng et al 2008) may also be tested in a new parameterization.

Light

Calcification is a light-dependent energy requiring process (Anning et al, 1996). The relationship between calcification and light is similar to photosynthesis (Nimer and Merret, 1993). Calcification is saturated ($>150 \mu\text{mol m}^{-2} \text{s}^{-1}$) at light levels generally lower than photosynthesis (Zondervan 2007) and there is some evidence of photo inhibition (less calcification at 400 than at $50 \mu\text{mol m}^{-2} \text{s}^{-1}$, Feng et al 2008). Calcification becomes limited by light to the extent that below a certain threshold value (e.g. $<150 \mu\text{mol m}^{-2} \text{s}^{-1}$, Zondervan et al 2002) there ceases to be an impact of changes in CO_2 on calcification (Zondervan et al 2002, Feng et al 2008). Dark calcification also occurs suggesting that photosynthesis and calcification are decoupled (Balch et al 1996), and is generally found to be 10 to 15% of the light saturated rate in short-term incubation experiments (Paasche, 2002). Incidentally, zinc limitation can also lead to decoupling between photosynthesis and calcification, with calcification unaffected by the lack of zinc (Schulz et al 2004). Cell growth limitation by light may also prolong the cell in the G1 phase and enhance the PIC cell content (Muller et al 08), which may partly explain dark calcification. The light used for calcification may be the PAR spectrum which is suggested by a single study (Paasche, 1966) in which absorption peaks for both calcification and photosynthesis occurred at the same red and blue wavelengths. However, as suggested by Paasche (2002), further experimental studies are needed to confirm these light dependencies. If confirmed, the light energy is likely to be harnessed through the chloroplast. In summary, it seems that calcification is a light dependent process (Paasche, 2002 and references therein) and as such light should be included in a new parameterisation of calcification.

CO_2

It is well established that the response of calcification to changes in CO_2 concentrations (or saturation state) is variable both in sign and magnitude (Ridgwell et al 2009). Most studies (e.g. Riebesell et al 2000, Zondervan et al 2001) show a decrease in calcite production with higher CO_2 levels while others show a different or opposite response (Langer et al 2006, Iglesias-Rodriguez et al 2008). The response may also be light dependent: below a threshold irradiance changes in calcite production were undetectable in contrast to higher light levels (Zondervan et al 2002, Feng et al 2008). Ridgwell et al (2009) summarises the CO_2 -calcification responses so far obtained from published studies and make the point that all ship-board and mesocosm experiments show an unambiguous direction to the response of calcification to CO_2 . On this basis (as well as other observations) they suggest that modelling integrated ecosystem calcification may be improved by analogy with the Eppley curve. If such an approach is valid, a relatively smooth ecosystem response to future changes in atmospheric CO_2 is likely to be one in which coccolithophore species transition from more to less heavily calcified strains. However, parameterisations for such a curve are currently not available and await future experimental work.

Building on the idea that most studies show that calcification decreases with a lowering in saturation state (Ridgwell et al, 2009), it would seem reasonable to include this effect in a model of calcification (Gehlen et al 2007).

2.2 Implementation

Towards a new model of calcification: user guide on how to adopt the equation

The following equation for calcification (13a) is based on the consideration from the literature described above. The novelty of the approach concerns the addition of phosphate:

$$Rc = P_{cocco} * C_{max} * R_f * T_{func} \quad 13a$$

Where limitation can be either multiplicative:

$$R_f = \underbrace{\left(1 - \frac{PO4}{PO4 + K_{po4}}\right)}_{\text{Phosphateinhibition}} * \underbrace{\left(\frac{I}{I + K_I}\right)}_{\text{Light limitation}} * \underbrace{\left(\frac{(\Omega - 1)}{(\Omega - 1) + K_{\Omega}}\right)}_{\text{saturationstatefactor}} \quad 13b$$

or a Leibig's minimum formulation:

$$R_f = \min \left(\underbrace{\left(1 - \frac{PO4}{PO4 + K_{po4}}\right)}_{\text{Phosphateinhibition}}, \underbrace{\left(\frac{I}{I + K_I}\right)}_{\text{Light limitation}}, \underbrace{\left(\frac{(\Omega - 1)}{(\Omega - 1) + K_{\Omega}}\right)}_{\text{saturationstatefactor}} \right) \quad 13c$$

The temperature function follows that of Eppley

$$T_{func} = e^{0.063T} \quad 13d$$

with an option to cap the temperature effect beyond 20°C (considering Langer et al 2006, and Feng et al 2008) i.e.

$$T_{func} = e^{0.063T} \text{ for } T \leq 20^{\circ}\text{C}, \text{ otherwise } T_{func} = e^{0.063*20} \quad 13e$$

The parameters are as follows (their values are shown in Table 2): K_{po4} is the half saturation for phosphate inhibition (set to be equal to the half saturation constant for phosphate-limited coccolithophore growth), K_I is the half saturation for light limitation, set to be approximately one quarter of the half saturation constant for light limitation of coccolithophore photosynthesis, after Tyrrell and Taylor, 1996) and K_{Ω} is the half saturation for saturation-limitation (Gehlen et al 2007).

2.2.1 Intercomparison of Calcification Parameterisations

Methods

In order to carry out an inter-comparison of the 12 parameterisations for calcification rate we first constructed a model to simulate the basic biogeochemistry (annual cycles of nitrate, phosphate, phytoplankton, zooplankton and detritus). To give a base model into which we could fit each calcification parameterisation in turn, this model was fitted to observations from an open ocean time series. This allowed us to compare the resulting cycles of DIC and alkalinity in a fair manner. More specifically, the configurations and parameter values for the base model remained the same for all 12 calcification parameterisations. We now discuss the details of the model.

Basic model

The base model simulates biogeochemistry in the mixed layer at an open ocean time-series site in the southern Bay of Biscay monitored by IEO Santander. This location was chosen for the inter-comparison because of the excellent time series of observations for all model variables bar detritus (more details on the site and data can be found below) plus availability of inorganic carbon measurements from the Ferrybox programme (details once more below). The model explicitly represents phytoplankton, zooplankton, detritus, nitrate and phosphate. For the first four variables the model units are mmol N m^{-3} . For the latter variable they are mmol P m^{-3} . The equations describing the model are based on those of Oschlies and Garçon (1998) modified to allow their use in a single layer model:

$$\begin{aligned} \frac{dP}{dt} &= J \cdot \frac{N}{k_N + N} \cdot P - \frac{g \cdot k_g \cdot P^2}{g + k_g \cdot P^2} \cdot Z - \mu_P \cdot P - P \cdot \frac{(V_{mix} + h^+)}{M} \\ \frac{dZ}{dt} &= \beta \cdot \frac{g \cdot k_g \cdot P^2}{g + k_g \cdot P^2} \cdot Z - \mu_{Z1} \cdot Z - \mu_{Z2} \cdot Z^2 - Z \cdot \frac{h}{M} \\ \frac{dD}{dt} &= (1 - \beta) \cdot \frac{g \cdot k_g \cdot P^2}{g + k_g \cdot P^2} \cdot Z + \mu_P \cdot P + \mu_{Z2} \cdot Z^2 - \mu_D \cdot D - D \cdot \frac{(V_{mix} + V_{snk} + h^+)}{M} \\ \frac{dN_n}{dt} &= -J \cdot \frac{N}{k_N + N} \cdot P + \mu_{Z1} \cdot Z + \mu_D \cdot D + (N_0 - N_n) \cdot \frac{(V_{mix} + h^+)}{M} \\ \frac{dN_p}{dt} &= \frac{1}{R_{np}} \cdot \frac{dN_n}{dt} + (P_0 - N_p) \cdot \frac{(V_{mix} + h^+)}{M} \end{aligned}$$

where P is phytoplankton, Z is zooplankton, D is detritus, N_n is nitrate, N_p is phosphate, M is mixed layer depth (m), $h = dM/dt$ and $h^+ = \max(h, 0)$. The last term on the right hand side of each equation represents the net loss from the mixed layer from the effects of mixed layer deepening (when $h > 0$), small scale turbulent mixing (at a rate parameterised as V_{mix}/M) and sinking due to gravity (at a speed V_{snk}). For simplicity, it is assumed that concentrations of phytoplankton, zooplankton and detritus below the mixed layer are negligible. It was further assumed that the motility of zooplankton allows them to avoid mixing and that only detritus sinks (i.e. that live phytoplankton can maintain their buoyancy). Sub-mixed layer concentrations of nitrate (N_0) and phosphate (P_0) are fixed at 6 mmol N m^{-3} and $0.4 \text{ mmol P m}^{-3}$ respectively. The mixed layer depth is taken from the output of a well-established freely available one-dimensional physical model (General Ocean Turbulence Model (GOTM) - <http://www.gotm.net/>) configured for the study site (Somavilla, R., C. González-Pola, C. Rodriguez, S. A. Josey, R. F. Sánchez, and A. Lavin (2009), Large changes in the hydrographic structure of the Bay of Biscay after the extreme mixing of

winter 2005, *J. Geophys. Res.*, 114, C01001, doi:10.1029/2008JC004974). We choose to use model output rather than monthly observations of mixed layer depth because of the strong influence on surface biogeochemistry of fluctuations in mixed layer depth, many of which would either be missed or smoothed out by monthly observations. To ensure accuracy of the physical model, it was run in a mode in which model fields were relaxed towards nearest hydrographic observations. A 20 day relaxation period was found to give the best agreement with observations. The light-limited maximum growth rate $J = J(I_0, V_p, \alpha, k_w, k_c, \phi)$ is calculated following Evans and Parslow (1985), where I_0 (Wm^{-2}) is the noon photosynthetically available radiation (PAR) at the surface on a given day, V_p is the maximum phytoplankton growth rate, α is the initial slope of the photosynthesis-irradiance curve, k_w is the attenuation coefficient for light in water, k_c is a self-shading attenuation coefficient and ϕ is latitude (used to calculate daylength using the standard astronomical formula). I_0 comes from observational data of surface irradiance taken at the study site. Note that J is the nutrient replete growth rate averaged over the mixed layer and over a daily period. The reader is referred to Evans and Parslow (1985) for more details. For the ratio of organic nitrogen to phosphorous we use the standard Redfield ratio of 16. Model parameter values can be found in Table 3. A description of how parameter values were chosen is given below.

The Spanish Institute of Oceanography (IEO) has maintained an oceanographic time series monitoring program (RADIALES project, www.seriestemporales-ieo.net) since the late 1980s comprising regular standard sections for hydrobiological sampling along the Spanish coast. Due to the rapidly deepening bathymetry, the outer station (8) at Santander ($44^{\circ}54'N$ $3^{\circ}53'W$) is at the base of the shelf, with a water depth of nearly 2500m, and can therefore be considered as effectively an open ocean time-series site. Observations of mixed layer nitrate, phosphate, zooplankton biomass and hydrographic parameters are available with monthly resolution as far back as 1992. Chlorophyll is also available but here we make use of chlorophyll as measured by sea surface colour as this gives a greater temporal resolution allowing us to form monthly averages rather than single measurements to give a more robust fit of the model. However, similar results are obtained if in situ chlorophyll measurements are used.

To obtain as good a match between observations and model in an objective manner, the model's 14 parameter values (bar cfrac) were originally calculated by fitting the model output to observations using the micro-genetic algorithm (Table 3). For those already acquainted with the approach, the optimisation was run with 18 'genotypes' (parameter sets) in each generation, for 5000 generations. Note that to avoid the need for a model 'spin-up' the initial conditions for nitrate, phytoplankton, zooplankton and detritus were also included in the fitting. Subsequent to this fitting exercise, which used time-varying sub-mixed layer concentrations of nitrate and phosphate, it was found that the sub-mixed layer values were unrealistically affecting the surface values, effectively relaxing them to observations. Accordingly this was replaced with constant values (as described above). A consequence was that short period fluctuations (few days) in mixed layer depth led to unrealistic oscillations in P and Z in the summer as the entrained deeper water had winter nutrient levels rather than summer ones. Consequently, an ad hoc remedy was applied whereby entrainment of sub-mixed layer waters was only allowed when the mixed layer was deeper than 25m. For the same reason (and because it has little impact in winter compared to entrainment) mixing (V_{mix}) is set to zero also. These changes give a more realistic situation though it means that the parameter values used can no longer be viewed as objectively fitted. Model output obtained using the chosen parameter values are shown in Figure 1, superimposed with observations. Note that data from 1992-2007 was used for the fit, but only results from 2004-2007 are shown in Figure 1 as plotting all years renders the details unclear. The years 2004-2007 are chosen as they overlap with the period of inorganic carbon measurements discussed later. It is seen that in general the model does a reasonable job, particularly for nitrate and phosphate. The former is the field of most interest as its drawdown is a major driver of the drawdown of DIC. Generally the model seems to capture the seasonal variability in timing and magnitude, though chlorophyll concentrations are clearly too low in summer. Introducing a non-zero but still small mixing rate remedies this but we choose not use it for the reasons given above.

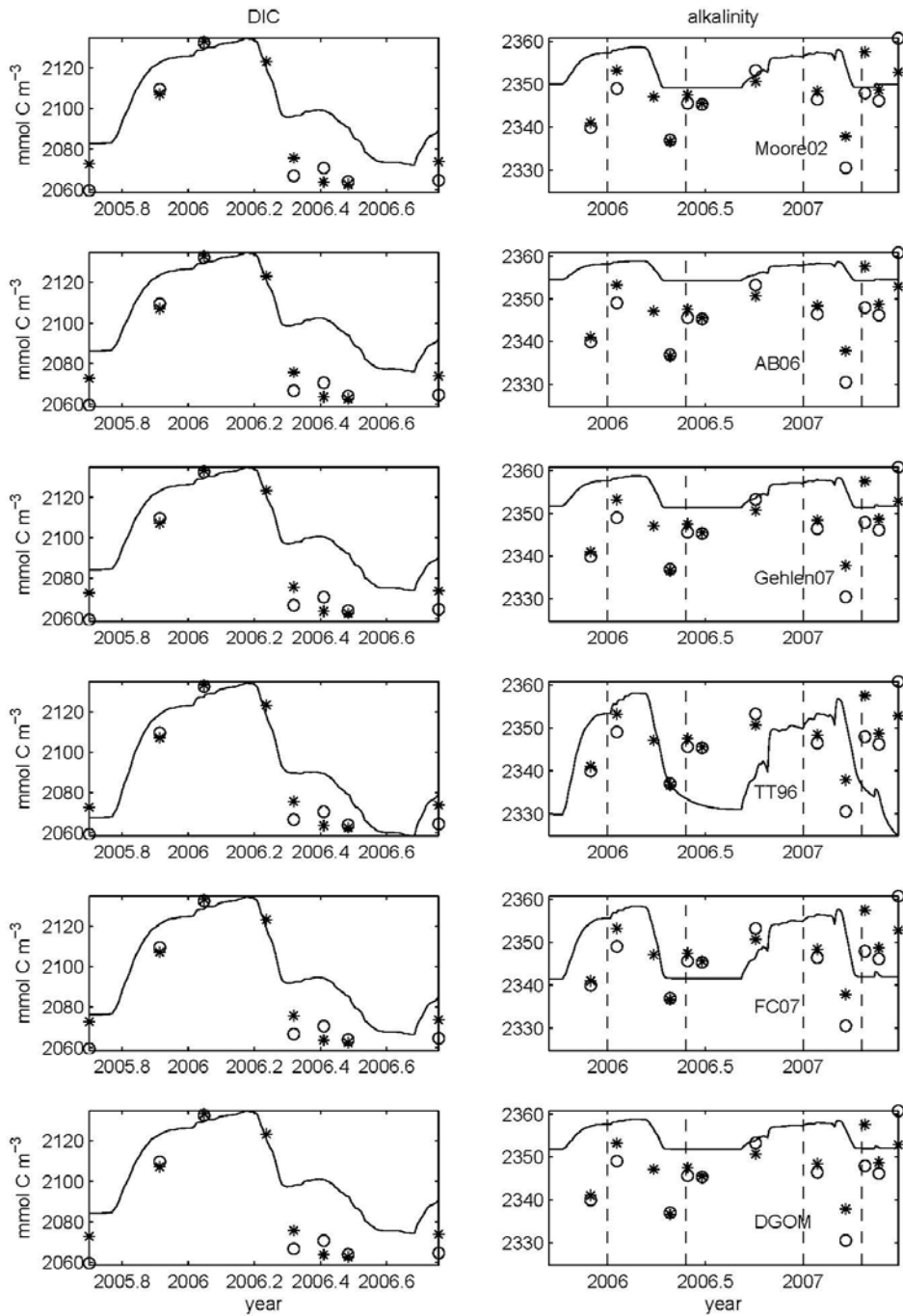


Figure 1: Model output (solid lines) and observations (circles) for the period 2004-2007.

Carbon model

In order to assess the different calcification parameterisations that have been collated here it is necessary to include carbon chemistry in the model. To this end, explicit equations for dissolved inorganic carbon (DIC) and alkalinity were added:

$$\frac{dC}{dt} = R_{cn} \cdot \left[-J \cdot \frac{N}{k_N + N} \cdot P + \mu_{Z1} \cdot Z + \mu_D \cdot D \right] + \xi + G + (C_0 - C) \cdot \frac{(V_{mix} + h^+)}{M}$$

$$\frac{dA}{dt} = -2 \cdot \xi + (A_0 - A) \cdot \frac{(V_{mix} + h^+)}{M}$$

where ξ is the calcification rate and R_{cn} is the Redfield ratio of carbon to nitrogen (106/16). G is the rate of air-sea gas transfer given by

$$G = V_{piston} \cdot k_H \cdot (pCO_2^{air} - pCO_2^{sea})$$

where V_{piston} is the piston velocity and k_H is the solubility of CO_2 at the instantaneous sea temperature and a reference pressure of 1atm. The solubility of CO_2 and also the calculation of other parameters of carbonate chemistry (including pCO_2^{sea}) from DIC and alkalinity were calculated using the *csys* routines³ (Zeebe & Wolf-Gladrow, 2001).

We use each of the previously discussed parameterisations for the calcification rate, ξ , in turn. As forcing we use observations of pCO_2^{air} from the nearest time-series site, Mace Head in Ireland (http://www.nuigalway.ie/ccaps/mace_head.html). For sub-mixed layer values, D_0 (2133 mmol C m⁻³) and A_0 (2359), we used largest winter values from surface observations in the Bay of Biscay on the assumption that mixed layer values are in close agreement with deeper values at this time. This was also done to set the sub mixed layer salinity used by the Friis (2007) parameterisation. The Bay of Biscay observations come from the Ferrybox project (http://www.noc.soton.ac.uk/ops/ferrybox_index.php) on the P&O Pride of Bilbao which makes regular crossings from Portsmouth, UK to Bilbao, Spain. Observations are averaged within two regions, north and south Bay of Biscay, to give more robust estimates. With a few gaps, these data are available monthly from September 2005 to July 2007. It is against these surface data that we will test the predictions of each of the calcification parameterisations.

2.2.2 Inter-comparison of calcification parameters

Each of the calcification parameterisations in turn was used to calculate \square in the above model. All forcings and other parameter values remained the same for all model runs. Two assumptions were made: first, that all of the calcification was carried out by phytoplankton; second, that these calcifying phytoplankton could be expressed as a fixed ratio of total phytoplankton. This ratio was taken to be 0.2 (Poulton pers. comm.). Future work may look at whether a better reproduction of observations can be obtained when explicitly modelling calcifying phytoplankton though it would bear the additional 'cost' of adding several degrees of freedom to the model with little quantitative data to constrain them.

Figures 2 and 3 show the model output for the period September 2005 to December 2006 for DIC (2007 data are still being quality checked) and September 2005 to July 2007 for alkalinity, superimposed with observations. It is seen that the annual drawdown of nitrate allows the models to capture the timing of DIC drawdown but that it does not progress far enough. This is because the observations indicate a DIC drawdown of ~70 mmol C m⁻³ for a nitrate drawdown of ~6 mmol N m⁻³ giving a ratio of nearly 12 compared to the standard Redfield ratio of 6.625 used in the model. For alkalinity the models do a better, though still poor, job of capturing the magnitude of variability and most capture the seasonal pattern of lower values in the spring and early summer though it should be noted that this is not terribly clear even in the observations. It is seen that nitrate drawdown is by far the dominant influence on DIC with calcification and air-sea exchange playing minor roles, with differences between parameterisations only really visible across the summer. For alkalinity the models produce more variable results. That of Moore 02 seems to have virtually no signal (though there is one there). In the former case this is a direct consequence of taking a much lower value for a key parameter (the ratio of calcification to calcifying phytoplankton's primary production) than other authors: they use 0.05 whereas DGOM

³ http://www.soest.hawaii.edu/oceanography/faculty/zeebe_files/CO2_System_in_Seawater/csys.html

uses 0.433. Generally, the models capture the decrease in alkalinity seen in spring though tend to remain too low over the summer months rather than rise again. That said, the seasonal cycle in observations is far from clear and so we will focus on the models' ability to capture the drop in alkalinity in spring. This key period for each year of observations is indicated with dotted lines in Figures 2 and 3. Both the TT96 and Friis 07 models do a good job of capturing this though at the cost of poorly reproducing summer values.

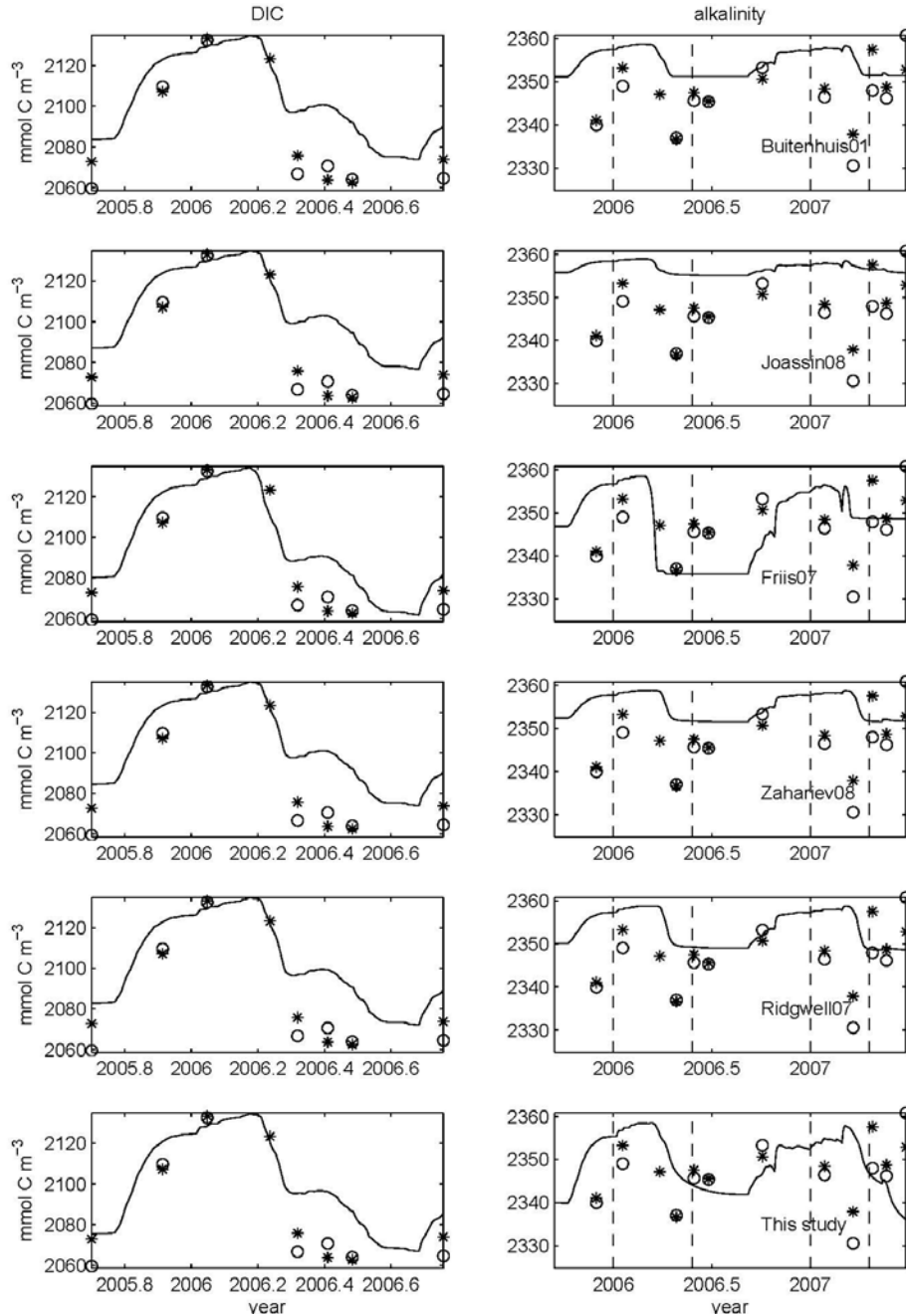


Figure 2:

Comparison of model output (solid lines) and observations (stars correspond to north Bay of Biscay and circles correspond to south Bay of Biscay) for DIC (left) and alkalinity (right). For ease of comparison, axes are the same for all models. The particular parameterisation is given in the lower right hand corner of the

alkalinity plot. The parameterisations compared here are: Moore 02, AB06, Gehlen 07, TT96, FC07 and DGOM.

Figures 2 and 3 show the model output for the period September 2005 to December 2006 for DIC (2007 data are still being quality checked) and September 2005 to July 2007 for alkalinity, with observations superimposed. It is seen that the annual drawdown of nitrate allows the models to capture the timing of DIC drawdown but that the amplitude of drawdown is insufficiently large. For alkalinity the models do a better, though still poor, job of capturing the magnitude of variability and most capture the seasonal pattern of lower values in the spring and early summer though it should be noted that this is not terribly clear even in the observations. This is because the observations indicate a DIC drawdown of $\sim 70 \text{ mmol C m}^{-3}$ for a nitrate drawdown of $\sim 6 \text{ mmol N m}^{-3}$ giving a ratio of nearly 12 compared to the standard Redfield ratio of 6.625 used in the model. It is seen that nitrate drawdown is by far the dominant influence on DIC with calcification and air-sea exchange playing relatively minor roles, with differences between parameterisations only really visible across the summer.

The performance of the different parameterisations can be assessed more quantitatively. For each parameterisation a misfit was calculated, defined as the root mean square difference between model and observations. To provide more detailed diagnosis, this misfit was calculated separately for both DIC and alk and for the north and south data. Details can be found in Table 4. For DIC, the models of TT96 and Friis 07 do best closely followed by those of this study and FC07 with the others bunched around 0.75-0.9. For alkalinity, the models which do least well are those of TT96 and Moore 02. The other models perform roughly equally well, with Friis 07 the exception, outperforming all others by a small but significant margin. The reason for the TT96 models' poor performance compared to how it reproduces DIC variability is the poor summer representation. If we instead focus on the spring drop in alkalinity then we get a different perspective (Table 5). TT96 does well. Only three other parameterisations do better – those of FC07, Friis 07 and this study. Although these 4 models most accurately capture the decrease they do not capture the absolute values during spring very well. In summary, the differing parameterisations of calcification can not be clearly separated on the basis of DIC observations as the dominant signal in DIC dynamics comes from nitrate dynamics which they all share. The various parameterisations do make strongly different predictions for alkalinity cycles. Choosing between them is a complex matter however: the absence of a 'clean' and strong seasonal cycle makes comparison of fit to the seasonal cycle potentially a weak test; focussing on specific criteria (e.g. spring drop in alkalinity) can give results contradicting those from simple root mean square fits; the underlying phytoplankton ecosystem model is far from perfect (e.g. chl values in summer); many models could almost certainly perform better if their parameters were tuned to the location rather than using the original literature values as we do here. Whether it would be justified to do the latter will take some consideration and is the topic of ongoing work.

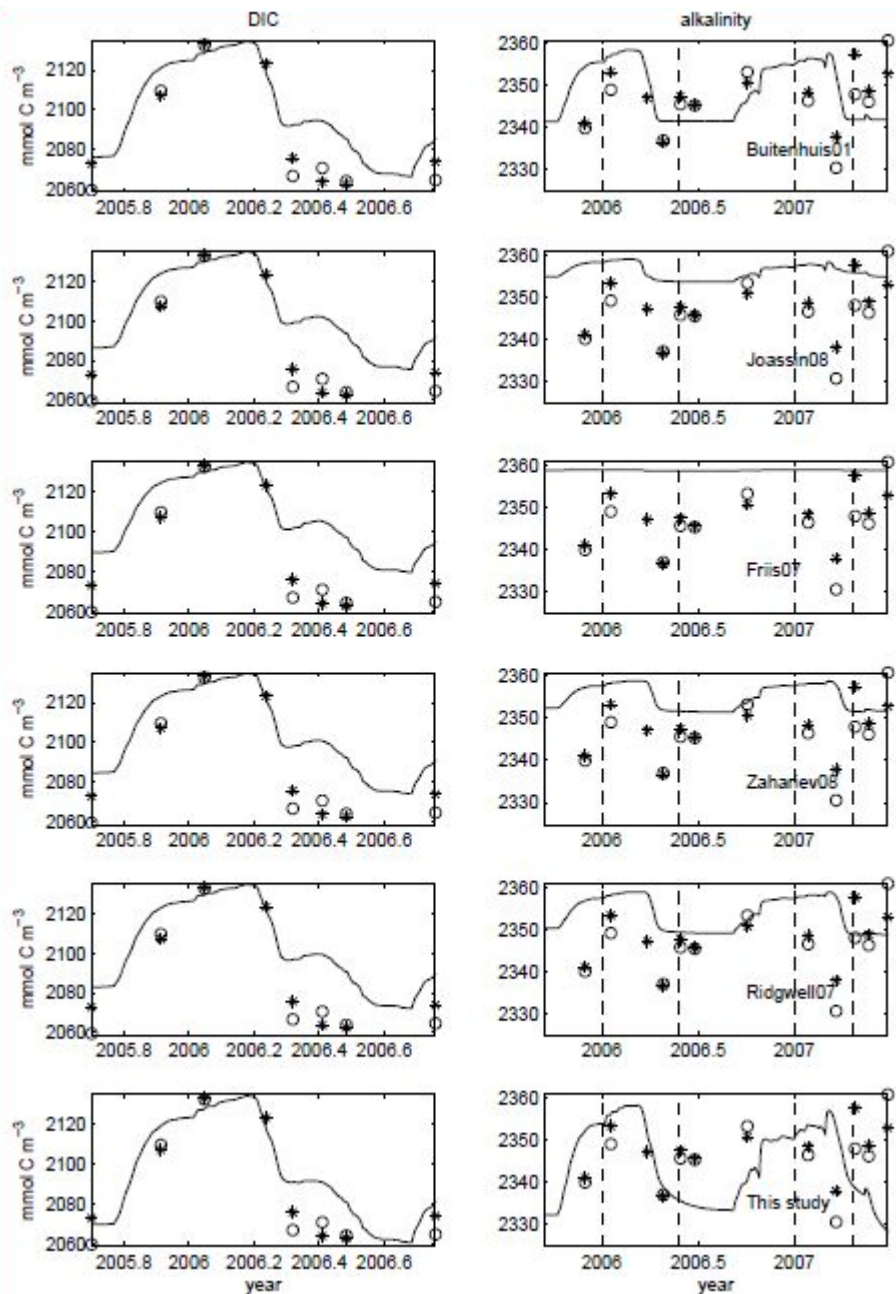


Figure 3: As figure 2 but for the parameterisations of: Buitenhuis 01, Joassin 08, Friis 07, Zahariev 08, Ridgwell 07 and this study.

References:

Evans, G. T. and J. S. Parslow (1985). A model of annual plankton cycles. *Biol. Oceanogr.*, 3, 327-347.

Oschlies, A. and V. Garçon (1998). Eddy-induced enhancement of primary production in a model of the North Atlantic Ocean. *Nature*, 394, 266-269.

Somavilla, R., González-Pola, C., Rodríguez, C., Josey, S.A., Sánchez, R.F. and Lavín, A. (2009). [Large changes in the hydrographic structure of the Bay of Biscay after the extreme mixing of winter 2005](#). *Journal of Geophysical Research*, 114, (C1), C01001. (doi:10.1029/2008JC004974)

Table 1: Major categories of calcification models and their equations.

Category 1 = based on primary production; = 2 based on export flux out of the euphotic zone; =3 based on phytoplankton biomass. G, R, M and F refer to global model, regional model, mesocosm model and field model, respectively. Note that the units for calcification are carbon, except in equation 9a which has nitrogen units. Symbols, variables and parameters defined in Table 2.

Category	Equation	Ref.
1G	$Rc = C_f * PP_{small} * (NUT_{LIM})^2 * \max\left(2, \frac{P_{small}}{2}\right) * f(T)$	¹ Moore02
	$NUT_{LIM} = \min(DIN_{lim}, P_{lim}, Si_{lim})$	1b
	$f(T) = \frac{T + 2}{28} \text{ for } T < 5^\circ\text{C}$	1c
	$f(T) = 0.0001 \text{ for } T < 0^\circ\text{C}$	1d
	$\text{else } f(T) = 1$	1e
1G	$C_{PIC:POC} = C_{PIC:POC}^m * NUT_{LIM} * \max\left(0.0001, \frac{T}{2+T}\right) * \max\left(1, \frac{P_{nano}}{2}\right)$	² AB06
	$0.01 \leq C_{PIC:POC} \leq 0.8$	2b
	$Rc = C_{PIC:POC} * PP_{nano}$	2c
1G	$C_{PIC:POC} = C_{PIC:POC}^m * \frac{(\Omega - 1)}{K_\Omega + (\Omega - 1)} * NUT_{LIM} * \max\left(0.0001, \frac{T}{2+T}\right) * \max\left(1, \frac{P_{nano}}{2}\right)$	³ Gehlen07
	$\Omega = \frac{[Ca^{2+}] * [CO_3^{2-}]}{k_{sp}}$	3b
	$Rc = C_{PIC:POC} * PP_{nano}$	3c
1G	$Rc = CP^{const} * PP_{cocco} * (1 - \delta_{DOC})$	⁴ DGOM
1R	$Rc = C_{PIC:POC}^{const} * R_{C:N} * PP_{cocco_N}$	⁵ FC07
1M	$Rc = \max(0, Cuptake - Resp) * C_{PIC:POC}^{const} + C_{basalrate} * P_{ehux}$	⁶ Joassin08
1G	$F_{PIC} = A * (PP_{total} - 0.5 * P_{BSi})$	⁷ Heinze04
	$F_{PIC} = A * F * (PP_{total} - 0.5 * P_{BSi})$	7b
	$F = 1 - (CO_2^{actual} - CO_2^{preindustrial}) * 0.012$	7c

1G	$F_{PIC} = A * r * (PP_{total} - 0.5 * P_{BSi}), r = f(\Omega)$	8a	⁸ Ilyina08
1R	$Rc = R_{PIC:POC}^{x,y} * P_{max} * \frac{I}{I + K_I} * \frac{PO_4}{PO_4 + K_{po4}}$	9a	⁹ Friis07
	$R_{PIC:POC}^{x,y} = \frac{1}{14.6} * \frac{P_{ALKd} - P_{ALKs}}{nNO3_d - nNO3_s}$	9b	
	$P_{ALK} = (ALK + NO3) \frac{35}{S}$ (salinity normalized ALK)		
	$nNO3 = NO3 * \frac{35}{S}$ (salinity normalized NO3)		
1FM	$Rc = C_{PIC:POC}^{const} * P_{ehux} * k_{calcif}$	10a	¹⁰ Buitenhuis01
	$k_{calcif} = \mu_{max}^{ehux}$ if time < delay period else		
	$k_{calcif} = \mu_{max} (t - delay)$		
	Where $\mu_{max} = \mu_{max}^{ehux} * \frac{NO3}{NO3 + K_{ehux}}$		
2G	$F_{PIC} = R_{C:N} * R_{PIC:POC} * F_{PON}$	11a	¹¹ Zahariev08
	$R_{PIC:POC} = R_{PIC:POC}^m * \frac{e^{(aci(T-T_{ci}^*))}}{1 + e^{(aci(T-T_{ci}^*))}}$	11b	
	$F_{PIC_{deep}} = F_{PIC} * \frac{1}{d_{PIC}} * e^{\left[\frac{(z-d_{eu})}{d_{PIC}} \right]}$	11c	
	$F_{PON} = \omega_S * D$	11d	
2G	$F_{PIC} = R_{PIC:POC} * F_{POC}$	12a	¹² Ridgwell07
	Where		
	$R_{PIC:POC} = r_{PIC:POC}^0 * (\Omega - 1)^\eta$	12b	
3R	$Rc = R_{C:N} * C_{max} * e^{0.063T} * \Psi(I) * P_{ehux}$	13a	¹³ TT96
	$\Psi(I) = \frac{1}{M} \int_0^M \frac{Iz}{I_{h,d} + Iz} dz$		

¹Moore et al 2002; ²Aumont and Bopp, 2006; ³Gehlen et al 2007; ⁴DGOM (B. Sinha, pers comm.); ⁵Fujii and Chai, 2007; ⁶Joassin et al 2008; ⁷Heinze, 2004; ⁸Ilyina et al 2008; ⁹Friis et al 2007; ¹⁰Buitenhuis et al 2001; ¹¹Zahariev et al 2008; ¹²Ridgwell et al 2007; ¹³Tyrrell and Taylor, 1996

Table 2: Variables, parameters and symbols used in the calcification equations shown in Table 1

Parameter Variable Symbol	Definition	Value	Reference
A	Tunable factor	0.15	Heinze 2004, Ilyina et al 2009
aci	Rain ratio scaling factor	0.6 K^{-1}	Zahariev et al 2008
$C_{basalrate}$	Calcification rate based on Ehux carbon biomass	0.024 d^{-1}	Joassin et al 2008
$C_{PIC:POC}^m$	Maximum cellular PIC:POC ratio	0.8	Gehlen et al 2007
$C_{PIC:POC}^{const}$	Fixed cellular PIC:POC ratio of coccolithophorids	0.4 $1 \text{ molC (molC)}^{-1}$ $2 \cdot 0.433$	A&B 2006 Fujii and Chai 2007
		0.58	Buitenhuis et al 2001
		0.5	Joassin et al 2008
C_f	Fraction of nanophytoplankton/coccolithophore primary production equal to calcification (=photosynthesis : calcification ratio)	0.05 0.433	Moore et al 2002 Moore et al 2002 (after Balch 2000) DGOM after Buitenhuis et al 01
C_{max}	Maximum rate of calcification/coccolith production	$0.2 \text{ mg cal C (mg orgC)}^{-1} \text{ d}^{-1}$	Tyrrell & Taylor 96; Merico et al 04 (after Fernandez et al 1993)
D	Detrital nitrogen		Zahariev et al 2008
δ_{DOC}	Fraction of coccolithophore primary production lossed to DOC leakage	0.05	B. Sinha, pers comm
F_{PON}	Detrital nitrogen flux out of the euphotic zone		Zahariev et al 2008
F_{POC}	POC flux out of the euphotic(?) zone		Ridgwell et al 2007
F_{PIC}	PIC flux out of the euphotic zone		Ridgwell et al 2007; Zahariev et al 2008; Heinze 2004
I_z	PAR level at depth z		
$I_{h,d}$	Half-sat. of calcification with respect to light	$40 \mu\text{Ein m}^{-2} \text{ s}^{-1}$ (9.6 W m^{-2}) 40 W m^{-2}	Tyrrell & Taylor 1996 Merico et al 2004
K_I	Half-sat for light limitation	$40 \mu\text{Ein m}^{-2} \text{ s}^{-1}$ (9.6 W m^{-2}) 40 W m^{-2}	Tyrrell & Taylor 1996 Merico et al 2004
K_{ehux}	Half-sat for P_{ehux} nutrient uptake	$0.1 \mu\text{M}$	Buitenhuis et al 2001
k_{sp}	Stoichiometric solubility product	$f(T,S,p)$	
K_{po4}	Half-sat. constant for phosphate uptake	$0.5 \mu\text{mol PO}_4 \text{ l}^{-1}$ $0.00025 \mu\text{mol PO}_4 \text{ l}^{-1}$ $0.2 \mu\text{mol PO}_4 \text{ l}^{-1}$	Friis et al 2007 Moore et al 2002
K_Ω	Half-sat. constant for saturation state limitation	0.4	Klausmeier et al 2004 Gehlen et al 2007

μ_{\max}^{cocco}	Maximum growth rate of coccolithophores	1 d ⁻¹	Fujii and Chai 2007
μ_{\max}^{ehux}	Maximum growth rate of P_{ehux}	0.69 d ⁻¹	Buitenhuis et al 2001
η	Power scaling for calcification response to Ω	<1.5	Ridgwell et al 2007
P_{BSi}	Biogenic silica production	Si units	Heinze 2004
P_{cocco}	Coccolithophore concentration	C units	Fujii and Chai, 2007
P_{cocco_N}	Coccolithophore N concentration	N units	
PP_{cocco}	Coccolithophore primary production	C units	
PP_{cocco_N}	Coccolithophore primary production	N units	Fujii and Chai, 2007
P_{ehux}	Emiliana huxleyi concentration	C units	Tyrrell and Taylor 1996, Merico et al 2004
P_{nano}	Nanophytoplankton carbon		Aumont and Bopp 2006; Gehlen et al 2007
PP_{nano}	Nanophytoplankton primary production	C units	Aumont and Bopp 2006
P_{small}	Nano- and pico-phytoplankton	C units	Moore et al 2002
PP_{total}	Total primary production	C units	Heinze 2004
P_{\max}	Max. community production	3 $\mu\text{M Phos y}^{-1}$	Friis et al 2007
$r_{PIC:POC}^0$	Spatially constant scalar for the PIC:POC rain ratio	0.044 (+0.038,-0.024) molC (mol C) ⁻¹	Ridgwell et al 2007
Rc	Rate of calcification of calcite		
$R_{C:N}$	C:N ratio of phytoplankton	6.625	
$R_{PIC:POC}$	PIC:POC rain ratio		
$R_{PIC:POC}^m$	Maximum PIC:POC rain ratio		See Table 3
T_{ci}^r	Rain ratio half-point temperature	10 °C	Zahariev et al 2008
Ω	Saturation state for calcite		
ω_s	Sinking rate of detritus	10 m d ⁻¹	Zahariev et al 2008
ω_{sed}	sedimentation rate of P_{ehux} and CaCO_3	0.02 – 0.12 d ⁻¹	Buitenhuis et al 2001
z	Depth		

¹combines mortality and metabolic losses

²for Ehux

Table 3: List of parameters and values used in the base model

Parameter	Units	Value
V_p	day ⁻¹	2.7556
α	W ⁻¹ m ² day ⁻¹	0.020079
k_w	m ⁻¹	0.04481
k_c	(mmol N m ⁻³) ⁻¹ m ⁻¹	0.039048
k_N	mmol N m ⁻³	0.48016
μ_P	day ⁻¹	0.034921
g	day ⁻¹	1.5635
k_g	(mmol N m ⁻³) ⁻² day ⁻¹	1.373
β		0.72381
μ_{Z1}	day ⁻¹	0
μ_{Z2}	(mmol N m ⁻³) ⁻¹ day ⁻¹	0.39365
μ_D	day ⁻¹	0.05873
V_{snk}	m day ⁻¹	13.5714
V_{mix}	m day ⁻¹	0.0
cfrac		0.2

Table 4: Misfit for each parameterisation compared to observations.

	DIC		alk		Mean
	north	south	north	south	
Moore 02	0.86	1.01	1.78	2.10	1.53
AB06	0.80	0.94	1.52	1.85	1.35
Gehlen07	0.75	0.89	1.36	1.69	1.23
TT96	0.48	0.54	1.99	2.27	1.55
FC07	0.60	0.70	1.30	1.59	1.12
DGOM	0.76	0.89	1.39	1.72	1.25
Buitenhuis 01	0.75	0.88	1.36	1.70	1.23
Joassin 08	0.82	0.96	1.58	1.92	1.39
Friis 07	0.54	0.63	1.25	1.50	1.06
Zahariev 08	0.76	0.90	1.46	1.77	1.29
Ridgwell 07	0.72	0.85	1.40	1.71	1.24
This study	0.63	0.73	1.43	1.80	1.25

Misfit is calculated as root mean square difference for each of the 4 datasets. Final value is mean of these 4. Note that each squared difference is normalised by the variance for the pooled north and south datasets. E.g. For DIC north,

$$misfit = \frac{1}{N} \sum_i \frac{(O_i - M_i)^2}{\sigma_{dic-NS}^2}$$

where N is the number of observations in DIC north dataset, O_i is the observation, M_i is the corresponding model output and σ_{dic-NS}^2 is the variance for the pooled north and south DIC datasets.

Table 5: Ratio of modelled spring decrease to observed decrease. The spring decrease period for each year is indicated by dashed lines in Figures 2 and 3.

	Model decrease:observed decrease		
	2006	2007	mean
Moore 02	0.07	0.06	0.06
AB06	0.28	0.24	0.26
Gehlen07	0.44	0.39	0.41
TT96	1.47	1.13	1.30
FC07	1.01	0.88	0.94
DGOM	0.42	0.36	0.39
Buitenhuis 01	0.45	0.39	0.42
Joassin 08	0.23	0.11	0.16
Friis 07	1.37	0.44	0.89
Zahariev 08	0.43	0.40	0.41
Ridgwell 07	0.57	0.56	0.56
This study	0.87	0.62	0.74

Table 6: Ratio of modelled spring decrease to observed decrease. The spring decrease period for each year is indicated by dashed lines in Figures 2 and 3.

	Model decrease:observed decrease		
	2006	2007	mean
Moore 02	0.07	0.06	0.06
AB06	0.55	0.48	0.52
Gehlen07	0.44	0.39	0.41
TT96	1.47	1.13	1.30
FC07	1.01	0.88	0.94
DGOM	0.42	0.36	0.39
Buitenhuis 01	1.01	0.88	0.94
Joassin 08	0.32	0.14	0.22
Friis 07	0.02	0.01	0.01
Zahariev 08	0.43	0.40	0.41
Ridgwell 07	0.57	0.56	0.56
This study	1.35	0.98	1.16

Section 3. Ocean acidification sensitivities and impacts

Jerry Blackford (PML)

3.1 Introduction

In collaboration with WP1 and other projects (e.g. EPOCA) parameterizations describing the impact of ocean acidification on marine biogeochemical processes are being developed. For processes that act at the organism level this is particularly problematic as significant species specific sensitivity has been observed. This document will be expanded as impacts emerge and are verified by the international community.

3.2 Nitrification

The following is a parameterisation of the impact of OA on nitrification, estimated from Heusemann et al, 2002 and previously applied in Blackford & Gilbert (2007). However this describes but one impact on the nitrogen cycle, where-as other parts of the nitrogen cycle are known to be sensitive. Using this formulation on its own will not necessarily tell you about how the N cycle will respond to OA.

In FORTRAN pseudo code:

```
Nitrification rate = nitrification rate * Min(2.0d0,Max(0.0d0, 0.6111d0*pH - 3.8889d0))
```

3.3 Calcification

Calcification is especially problematic as many different floral and faunal groups exhibit calcification, using different physiological mechanisms, each with different sensitivities. Underlying this there is significant species specific variability. See Fabry 2008 for discussion. Currently there is no recommendable parameterization for calcification.

References

- Blackford, J.C., Gilbert, F.J., 2007. pH variability and CO₂ induced acidification in the North Sea. *Journal of Marine Systems* 64, 229–241.
- Fabry, V.J. 2008. Ocean science - Marine calcifiers in a high-CO₂ ocean *Science*, 320, 1020-1022.
- Huesemann, M.H., Skillman, A.D., Crelius, E.A., 2002. The inhibition of marine nitrification by ocean disposal of Carbon dioxide. *Marine Pollution Bulletin* 44 (2), 142–148.